Independent component analysis for preprocessing optical signals in support of multi-user communication

Federica Aveta[a], Hazem H. Refai[a], Peter LoPresti[b], Sarah A. Tedder[c], Bryan L. Schoenholz[c]
[a]Department of Electrical Engineering, University of Oklahoma, Tulsa, USA
[b]Department of Electrical Engineering, University of Tulsa, Tulsa, USA
[c]NASA Glenn Research Center, Cleveland, Ohio, USA

ABSTRACT

Free Space Optical (FSO) communication is widely recognized for its powerful features, especially when compared to other wireless technologies utilized in point-to-point communication links. Although current literature focuses primarily on point-to-point transmission, multi-user FSO systems are beginning to draw significant attention. The primary objective in a multi-user communication system is to estimate individually transmitted signals from received signals, namely Blind Source Separation (BSS). A solution to the BSS problem in an FSO multi-user communication link is proposed. A multi-point FSO system composed of two independent transmitters operating at different wavelengths and a dual path fiber bundle receiver was used. The FastICA algorithm was exploited for multi-user detection. Experimental results demonstrate that this method can separate original transmitted signals from their received mixtures. Effects of signal power, data rate, misalignment error, and turbulence severity on signal separation are also explored to define the working range for achieving best performance.

Keywords: BSS, ICA, FSO, FastICA

1. INTRODUCTION

Wireless communications have benefitted tremendously from recent technological improvements and enjoyed rapid growth. Consequently, increasing usage and higher demand for wireless traffic are causing a critical need for increased bandwidth and capacity. Optical wireless communication (OWC) proves promising for high speed and broadband connection[1] and it offers several advantages over current RF (radio frequency) technology. In particular, Free Space Optical (FSO) technology has a large optical bandwidth available (e.g. order of THz), allowing much higher data rates (e.g. actual transmission rate up to 10 Gbps). FSO systems use a highly directional beam with very narrow beam divergence, offering high security against interception and eavesdropping while also adding robustness to electromagnetic interference. Furthermore, FSO is a license-free technology requiring less power and mass, which makes the communication system quickly and easily deployable at a low initial set up cost[2].

The increasing demand of mobile platforms and high-speed communication between them requires considerable improvement over current FSO system designs. Emerging FSO transceivers incorporate different designs (e.g., fiber-bundle) to enlarge the transceiver's field of view (FOV)[3]. While an increased viewer angle reduces errors due to misalignment between transmitter and receiver, and mitigates the effects of atmospheric turbulence, the wide aperture is at risk of receiving several optical signals simultaneously. This potential drawback can be leveraged, however, to implement a FSO multi-point communication link in which users transmit various signals that mix in a propagation medium and are collected by receivers. Although FSO has enjoyed widespread notoriety in fixed and point-to-point communication links, its use for multi-user scenarios is limited in current literature[4].

Blind Source Separation (BSS) estimates source signals from observed mixtures sans information about the mixing process and original signals[5]. Independent Component Analysis (ICA) is the most widely used method for performing BSS, as it is an unsupervised technique relying on simple assumptions based on signal statistical properties[6]. Statistically independent sources are assumed with one Gaussian distribution, at most. ICA is widely used in robotics, biomedical signal processing, speech processing, and wireless communication. In RF wireless communication, ICA has been used for wireless sensor networks (WSNs), cognitive radio networks (CRNs), multiple input and multiple output systems (MIMO), and code division multiple access (CDMA)[7]. This paper extends the use of ICA in OWC for multi-user detection in a multi-point system. FastICA, a well-known ICA algorithm, estimates directions for maximizing the

component's non-Gaussianity by utilizing negentropy or kurtosis as measure of non-Gaussianity. In particular, the FastICA algorithm is often used in real-world applications due to its high performance and fast convergence.

The FastICA algorithm was leveraged for multiuser detection on a multi-user optical system composed of two independent optical transmitters operating at 1310 nm and 1550 nm wavelength, two identical receivers (i.e., photodetectors), and a free-space turbulence simulation box. After proof of concept for signal separation[11], effects of signal power, data rate, misalignment, turbulence severity on signal separation, and signal demodulation were analyzed.

The balance of this paper is organized as follows. Section 2 describes the ICA statistical method and briefly introduces the FastICA algorithm used in this work. Section 3 describes the experimental setup and data collection. Section 4 details the results and offers analyses. Finally, Section 5 concludes the paper and states possible future work.

2. INDEPENDENT COMPONENT ANALYSIS: FASTICA

2.1 Independent Component analysis

The ICA model assumes N transmitters that transmit signals $s_1(t)$, $s_2(t)$, …, $s_N(t)$ and M receivers that observe signals $x_1(t)$, $x_2(t)$, …, $x_M(t)$, which are linear and instantaneous mixtures of the original sources. Therefore, the ICA model can be written as follows[6]:

$$x = As \tag{1}$$

where $x=[x_1, x_2, \ldots, x_M]^T$ is the observed mixtures vector; $s=[s_1, s_2, \ldots, s_N]^T$ is the unknown source signals vector; and $\mathbf{A}$ is the m x n unknown mixing matrix. The problem becomes estimating the original components $\mathbf{s_i}$ and the matrix $\mathbf{A}$ by knowing only the mixed received signals. The model is based on three assumptions. First, original source signals s_i should be statistically independent. Second, original sources $\mathbf{s_i}$ with only one exception should not have Gaussian probability distribution, allowing an estimate for mixing matrix $\mathbf{A}$. Notably, higher order statistics (HOS) are always zero for Gaussian distribution. However, these distributions are considered unknown. Third, for simplicity, the mixing matrix $\mathbf{A}$ is assumed nonsingular and square (i.e. the number of transmitter is equal to the number of receivers).

When estimating the mixing matrix, its inverse $A^{-1}=W$ is computed, where W represents the un-mixing matrix. Accordingly, independent components $\mathbf{s_i}$ are retrieved, as follows:

$$s = Wx \tag{2}$$

This solution is characterized by some ambiguities. The scale ambiguity states that determining independent component variances is impossible; thus, ambiguities in component magnitude and sign. Given that s_i and A are unknown, any scalar multiplied in sources s_i can be deleted by dividing for respective column a_i of A by the same scalar α_i:

$$x = \sum_i \left(\frac{1}{\alpha_i} \cdot a_i \right) (\alpha_i \cdot s_i) \tag{3}$$

Permutation ambiguity states that determining the order of the independent components is impossible. In fact, in Eq. 3 it is possible to change the order of the terms and to consider any independent component as the first one. Moreover, Eq. 1 can be rewritten, as follows:

$$x = AP^{-1}Ps \tag{4}$$

where $\mathbf{P}$ is the permutation matrix and $\mathbf{P^{-1}}$ is its inverse. Thus, elements of $\mathbf{Ps}$ are the original independent components in another order, and $\mathbf{AP^{-1}}$ is a new unknown mixing matrix. It is important to know that although these ambiguities don't represent a crucial problem in the instantaneous ICA model, the affect must be considered and solved for in other applications (e.g., in convolutive mixtures of source signals where time delays are involved during the mixing process)[12].

2.2 FastICA algorithm

The FastICA algorithm is an HOS method for BSS solution that aims to estimate directions for maximizing the non-Gaussianity of the original components by using a fixed-point iteration scheme. Accordingly, negentropy J is utilized as a quantitative measure of non-Gaussianity of a random variable[13]:

$$J(y) = H(y_{gauss}) - H(y) \tag{5}$$

where H is the differential entropy; y is a random vector; and y_{gauss} is a Gaussian random vector with the same covariance of y. Since Gaussian variables have the largest entropy among all random variables of equal variance, negentropy will be zero for variables with Gaussian distributions and non-negative for other distributions. Due to difficulties associated with computing negentropy, because it requires knowledge of probability distribution function of the data, approximations were used and were based on non-linear functions G and it is expressed as follows:

$$J(y) \propto [E\{G(y)-E\{G(v)\}]^2 \quad (6)$$

where v is a Gaussian variable of zero mean and unit variance, and G is a non-linear function.

The FastICA algorithm works on data requiring a two-step pre-processing. The first is centering (i.e., observed signal, x is centered by subtracting its mean value). The second is whitening (i.e., centered signal should be linearly transformed in a white vector whose covariance matrix is the identity matrix). This process lowers solution complexity due to the reduced number of parameters (i.e.., from n^2 to $n(n-1)/2$). The FastICA algorithm can be applied after pre-processing. This one-unit algorithm aims to maximize negentropy in Eq. 6, evaluated in $y=w^Tx$. Hence, optimum $E\{G(w^Tx)\}$ under constraint $E\{(w^Tx)^2\} = \|w\|^2=1$ can be found using the Lagrange function. The final solution is expressed, as follows:

$$w = E\{xg(w^Tx)\} - E\{g'(w^Tx)\}\, w \quad (7)$$

where g and g' are the first and second order derivative of G function. This algorithm—compared to other methods—has several advantages: it is extremely fast converging (e.g., cubic or at least quadratic); it possesses non-Gaussian distribution; and its distribution estimation is not required.

3. EXPERIMENTAL SETUP

The FSO experimental setup used in the research reported in this paper is shown in Fig. 1.

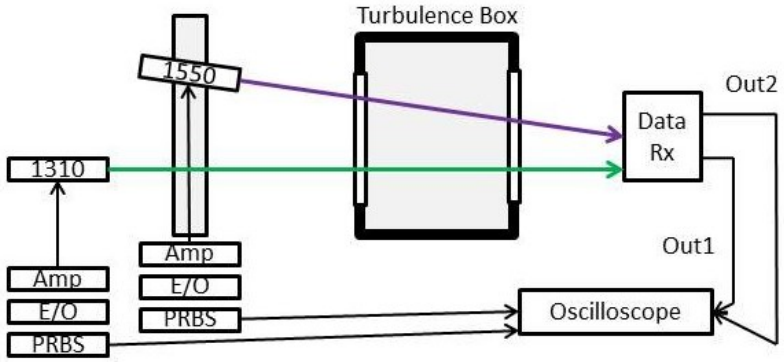

Figure 1. Depiction of experimental setup

Two independent optical sources were used: a 1550 nm and 1310 nm fiber coupled laser diodes. These diodes were driven by two independent pseudo-random bit sequences (PRBS) with 2^{31}–1 bits in length and various bit rates were tested. The 1550 nm optical output was connected to a doped fiber optical amplifier, and the 1310 nm to a semiconductor optical amplifier. The 1310 nm beam traveled parallel to the receiver's optical axis, and the 1550 nm beam traveled at an angle of 10 degrees relative to the receiver's optical axis. This angled transmitter was mounted on a translational platform for studying signal separation quality in the presence of misalignment errors. The turbulence box was equipped with an electrical heater and a variable ventilation aperture to control atmospheric turbulence within the box. To characterize turbulence, a beam profiler (e.g., Spiricon LT665-1550) was used to capture and analyze the beam shape coming out of the 1550 nm laser diode. Fig. 2 shows two independent transmitters (left) and the fiber bundle based receiver— a design reported in[3] (right). The receiver is composed of a hexagonal array of small lenses (e.g., f=3 mm) that couple the signal in an array of nineteen fibers (e.g., core diameter 400 μm). Outputs from the array are coupled through lenses to the collecting area of two photodetectors. The mixed signal was received by the fiber bundle end point and conveyed to two photodetectors via the fibers. Ten fibers of the bundle were coupled to photodetector one and nine fibers coupled to photodetector two. A 10° wedge prism was placed in front of the receiving lens array to vary the angle between the optical signals received by photodiode one and two. Each bundle efficiently collected light over a ±5° range

and experienced reduced coupling efficiency beyond this range. Transmitter beam diameters were adjusted such that optical power coupled efficiently into one set of fibers and coupled inefficiently with a loss into the other set of fibers.

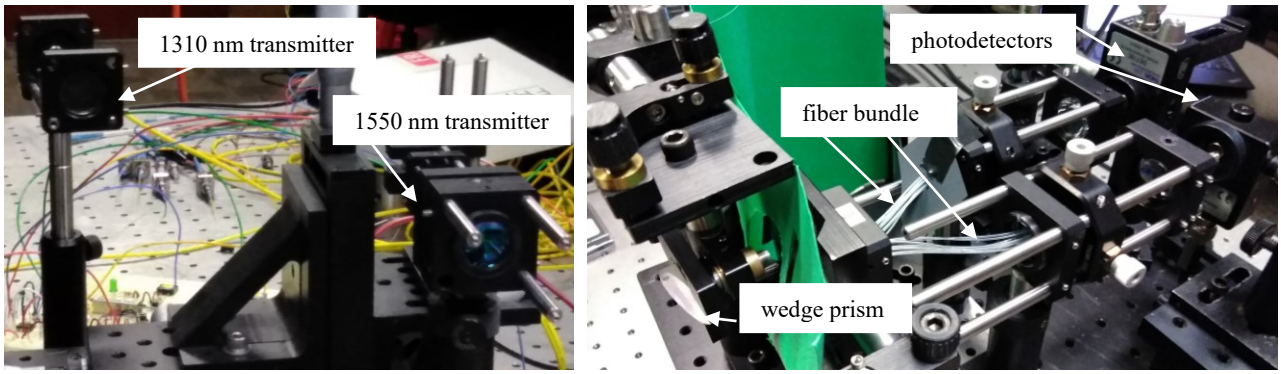

Figure 2. (left) Two independent transmitters and (right) the fiber-bundle receiver.

A National Instruments Virtual Bench, 4-channel oscilloscope was used to record data collected from the two photodetectors and the transmitted PRBS. The beam profiler Spiricon LT665-1550, consists of a phosphor coated CCD camera in the NIR wavelengths (i.e., 1440 nm-1605 nm) with an active area of 12.5 mm x 10 mm and pixel pitch of 50 μm. It has a USB 3.0 PC interface that allows the camera to be controlled by the analysis software BeamGage. The beam profiler was used to compare the laser beam without turbulence with the beam in presence of turbulence.

4. RESULTS

In a previous work, the effectiveness of the FastICA algorithm for signal separation has been reported[11]. Here, detailed analysis was performed to understand how signal power, data rate, misalignment errors, and atmospheric turbulence affect the quality of the signal separation. Two parameters were used for performance evaluation: performance index (PI) and signal interference ratio (SIR). PI is given by[14]:

$$\mathrm{PI} = \sum_{i=1}^{N}\left(\frac{\sum_{k=1}^{N}\left|q_{ik}\right|^2}{\max_p\left[\left|q_{ip}\right|^2\right]}-1\right)+\sum_{k=1}^{N}\left(\frac{\sum_{i=1}^{N}\left|q_{ik}\right|^2}{\max_p\left[\left|q_{pk}\right|^2\right]}-1\right) \tag{8}$$

where q is the element of the matrix Q=WA. Given a good separation, PI is near zero. SIR is expressed as follows[15]:

$$\mathrm{SIR} = 10\log\left[E\left\{\left(\left|y\right|_{\sigma(j),j}\right)^2\right\}\Big/E\left\{\sum_{k\neq j}\left(\left|y\right|_{\sigma(j),k}\right)^2\right\}\right] \tag{9}$$

Eq. 9 indicates the amount of useful signal on the j^{th} channel relative to other components considered as interfering signals. Hence, a higher value of SIR for the j^{th} channel is desired.

4.1 Power selection

Optical outputs from the two laser diodes were connected to a doped fiber optical amplifier (1550 nm) and to a semiconductor optical amplifier (1310 nm). The first amplifier has a power range from 6 dBm to 14 dBm, and the second one from 3 dBm to 15 dBm. To determine power values characterized with the best signal separation, all the power levels were tested. Initially, 1550 nm output power was set to the highest value, as it was the angled transmitter. The 1310 nm output power range was explored with a step of 3 dBm. After determining the power value while guaranteeing the lowest PI, the 1310 nm power level was fixed to that level, and the 1550 nm output power was set with step of 2 dBm. Power pair values were found to achieve optimal separation when set to 14 dBm for the 1550 nm transmitter and 9 dBm for the 1310 nm transmitter. These values correspond to the minimum PI measured (e.g., approximately 0.2). This result is shown in Fig. 3:

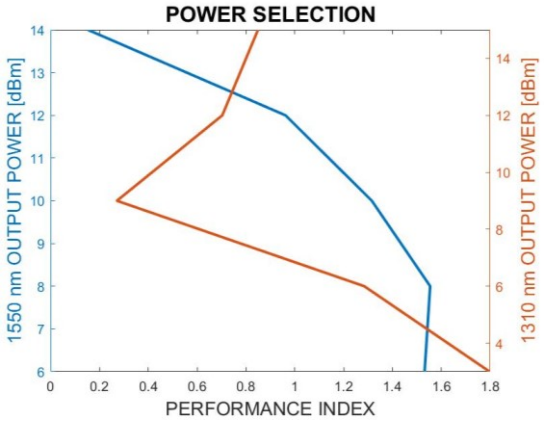

Figure 3. Power selection: Output power 1550 nm (blue line) and 1310 nm (orange line) versus Performance Index.

These optimum power values were used throughout the experimentation.

4.2 Data Rate

Data rate analysis was limited by the bandwidth of the photodetectors. Hence, testing was limited to 50 Hz – 400 Hz. Fig. 4 shows results for performance index (PI) and signal interference ratio (SIR) versus data rate.

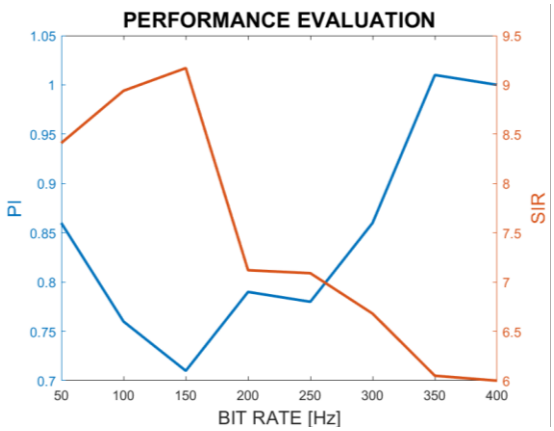

Figure 4. Performance evaluation: PI (blue line) and SIR (orange line) versus bit rate.

Fig.4 demonstrates how PI decreases and SIR increases up to 150 Hz, and then each trend changes, indicating that the quality of signal separation increases with bit rate. In fact, quality performances most likely decrease, beyond 150 Hz, due to slow speed photodetectors.

4.3 Misalignment

Misalignment either severs optical link, if severe, or reduces received optical power. A fiber bundle based receiver is considered a promising design for mobile FSO communication primarily because the increased FOV reduces the effect of misalignments on optical link. To test its effect a translational misalignment between the angled transmitter (1550 nm) and the receiver was adjusted with step of 1 cm until the point at which there was complete misalignment. Fig. 5 demonstrates separation resulting from a misalignment of 2 cm. Fig. 5 on the left illustrates the received mixed signals from photodetector one (i.e., green line) and from photodetector two (i.e., cyan line). Fig. 5 on the middle and on the right, represent the reconstructed source signals (i.e., blue lines) and the original transmitted signals (i.e., red lines). Notably, although we get a particularly noisy received signal, the algorithm is able to separate the mixed signals. In fact, both reconstructed signals have the same waveform as the original transmitted sources. Therefore, separation was considered acceptable even under misalignment conditions (e.g. PI=0.0515 and SIR=18.9038).

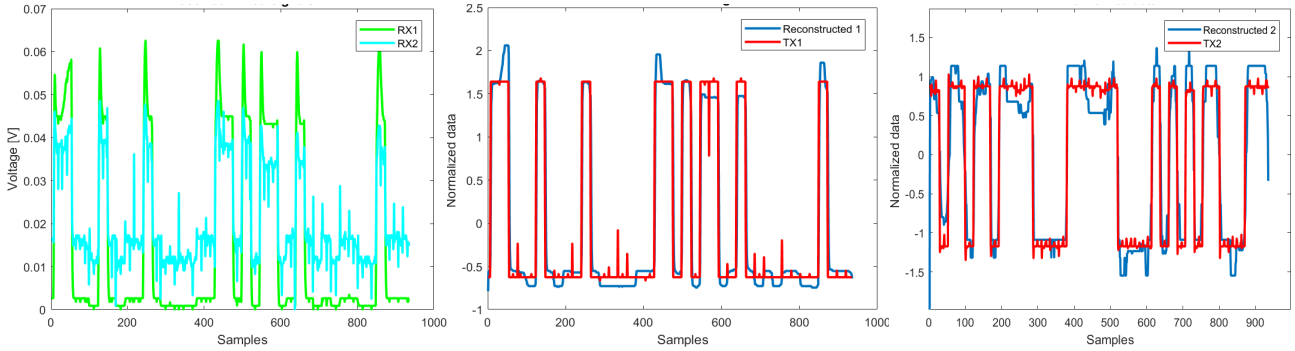

Figure 5. 2 cm translational misalignment: (left) The two received signals, (middle) the reconstructed signal 1, (right) the reconstructed signal 2.

4.4 Turbulence

Before utilizing the turbulence box to collect data, atmospheric turbulence was investigated on the propagation of the optical beam using the beam profiler. The beam profiler was placed behind the turbulence box (i.e., 30 cm far from the 1550 nm laser diode), with the camera plane orthogonal to the beam propagation direction. We collected and recorded data for 5 minutes. Fig. 6 depicts one frame of the 1-D, 2-D and 3-D beam profile of the 1550 nm laser diode without turbulence. The optical signal profile clearly shows that the beam is Gaussian, albeit quite distorted due to diffraction introduced by the transmitting lenses and noise in the lab environment. A least square bivariate normal equation (Gaussian equation) fitting in 1-D and 2-D was performed using Beam Gage Software. Hence, additional parameters were considered, including total power of the laser beam, Gauss centroid along X and Y, and roughness of fit. Mean and standard deviation of the obtained values and their explanations are shown in Table 1.

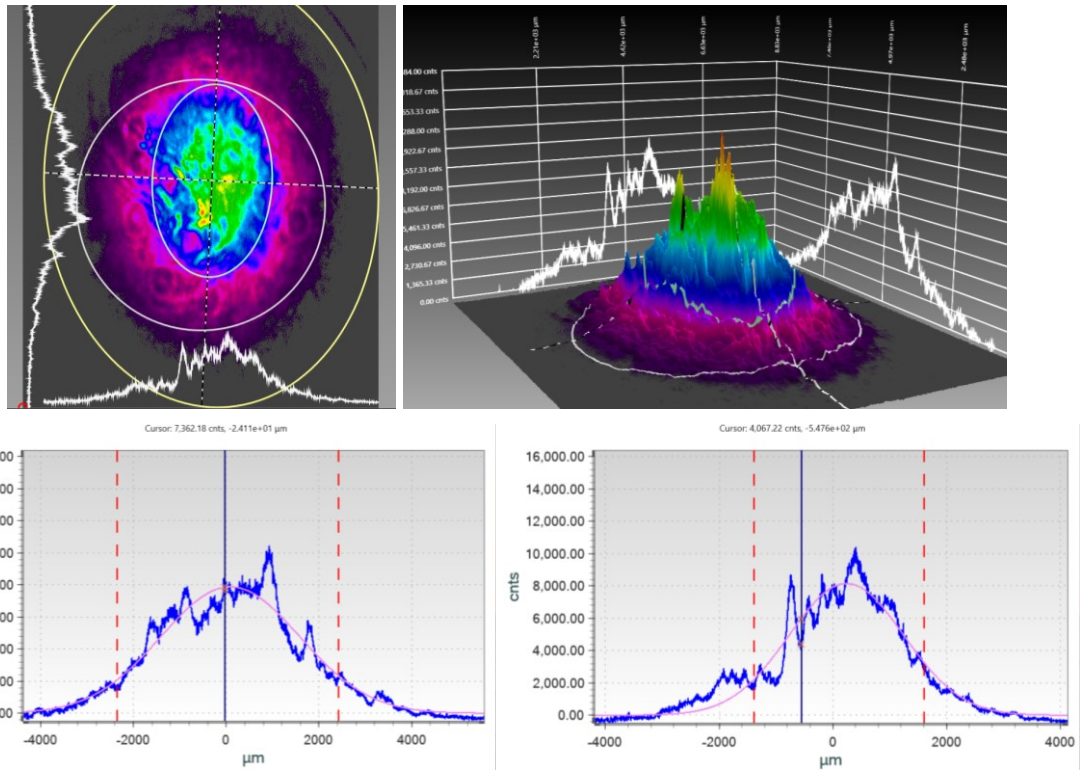

Figure 6. No turbulence beam profile: (upper left) 2-D and (upper right) 3-D beam profile, (bottom left) 1-D beam profile with fitting along Y axis and (bottom right) X axis .

Next, we turned on the electric heater in the turbulence box and waited until the box reached stable temperature before making measurements using the beam profile. Fig. 7 depicts one frame of the 1-D, 2-D and 3-D beam profiles of the 1550 nm laser diode with turbulence:

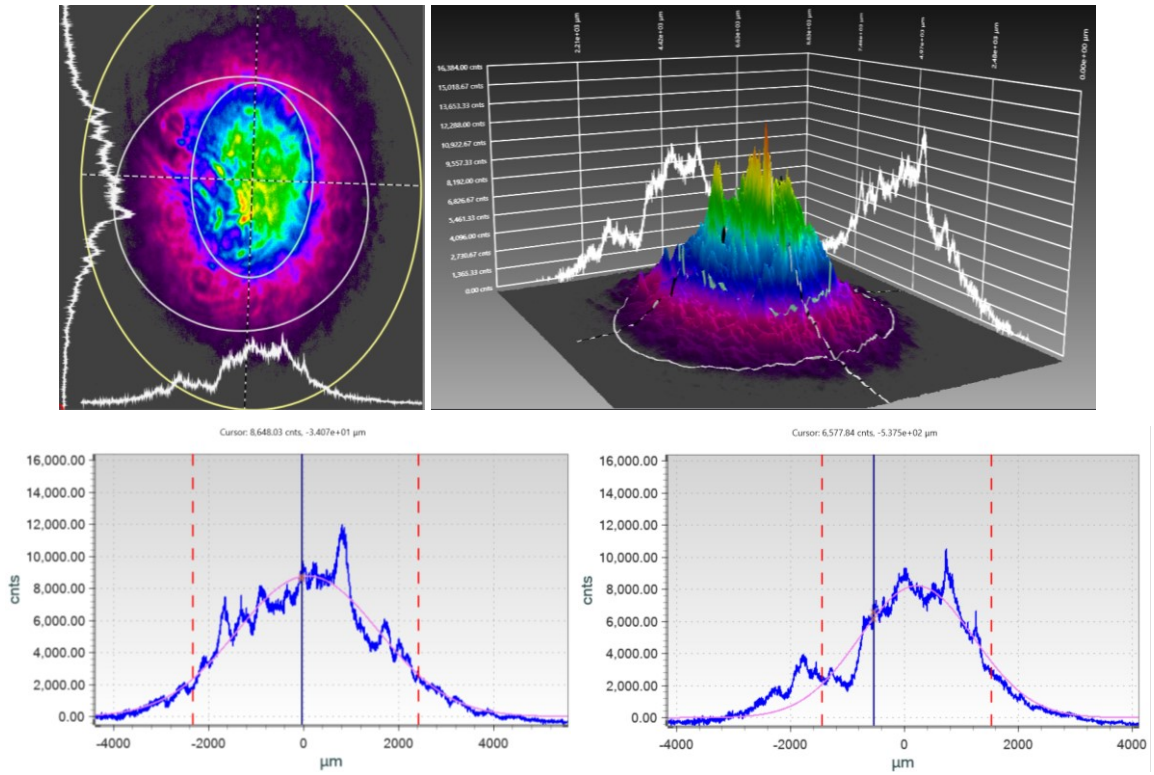

Figure 7. Turbulence beam profiler: (upper left) 2-D and (upper right) 3-D beam profile, (bottom left) 1-D beam profile with fitting along Y axis and (bottom right) X axis.

Although results under turbulence appear quite similar to those of non-turbulence (i.e. 3-D, 2-D and 1-D beam profile), comparing total power of laser, Gauss centroid along X and Y, and roughness of fit it is important to note the way in which turbulence is affecting the beam. Obtained values are shown in Table 1. By comparing values with those without turbulence, the effects of turbulence are limited but with higher standard deviation. This indicates that the beam is fluctuating to a greater extent, not only in intensity, as expected, but also in position around the fitted centroid. Moreover, roughness of the fit (i.e., deviation of the theoretical fit to the measured distribution) is increased both in mean value and standard deviation. Roughness of fit R should theoretically have a value between 0 and 1 and correspond with good fit and bad fit, respectively. Hence, an increase in mean value of roughness means a worsening in fit, and an increase in standard deviation means higher fluctuation in the signal.

Table 1. Fit parameter beam profile without turbulence on the fourth column and with turbulence on the third column.

Parameter	Definition	Mean+Std Value TURBULENCE	Mean+Std Value NO TURBULENCE
Total power	Total power of the laser beam (counts)	3.81E+09 ± 1.29E+08 [cnts]	3.65E+09 ± 2.59E+07 [cnts]
Gauss centroid along X	X coordinates of the fitted centroid	4773.731 ± 9.41 [µm]	4768.494 ± 1.87 [µm]
Gauss centroid along Y	Y coordinates of the fitted centroid	5520.001 ± 14.4 [µm]	5538.63 ± 1.37 [µm]
Roughness of the fit	Maximum deviation of the theoretical fit to the measured distribution.	0.727 ± 0.157	0.519 ± 0.012

Although the box introduced atmospheric turbulence, visible in the higher fluctuation of the laser beam, it can be considered as a small turbulence level.

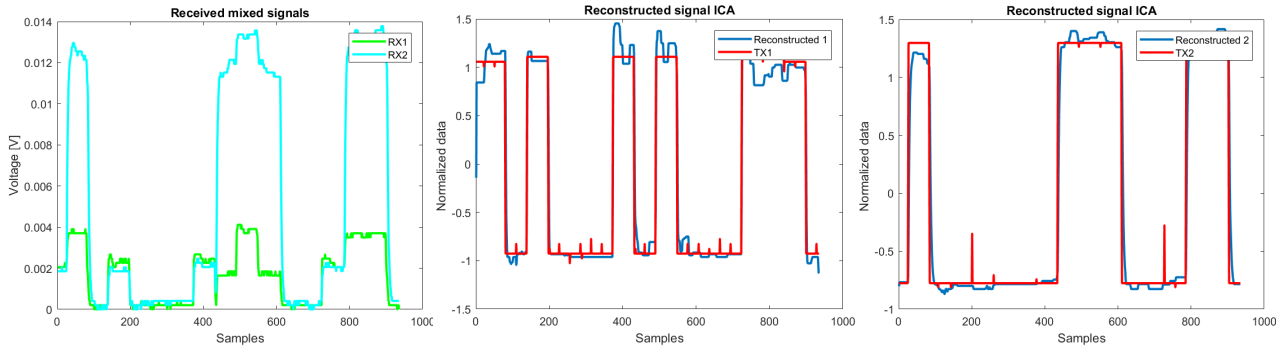

Figure 8. Turbulence case: (left) The two received signals, (middle) the reconstructed signal 1, (left) the reconstructed signal 2.

FastICA was again applied to test for signal separation under turbulence conditions. Fig. 8 illustrates one frame of the collected data. The left graph shows the received mixed signals from photodetector one (i.e., green line) and from photodetector two (i.e., cyan line) in the presence of turbulence; the middle and right graphs show the reconstructed source signals (i.e., blue lines) and the original transmitted signals (i.e., red lines). Notably, signal separation was acceptable even under turbulent conditions (e.g. PI=0.1916 and SIR=13.2916).

5. CONCLUSION

Independent Component Analysis (ICA) is an unsupervised signal processing technique widely used in wireless communication for a variety of applications. In this work, the FastICA algorithm—one of the most widely used for blind source separation—was employed for multi-user detection in an FSO communication link. The FSO system was composed of two independent transmitters, a dual path fiber bundle receiver and a turbulence box, that simulated atmospheric turbulence. Effects of varying power level, data rate, misalignment degree, and turbulence level were investigated. After having determined the optimum value for transmitted power and data rate, ICA proved suitable for source separation even in presence of translational misalignment and small atmospheric turbulence. Results confirm a method that can be successfully implemented for FSO multi-user communication. Although higher turbulence levels should be investigated in future work.

One of the most important conditions of ICA is that the number of receivers should equal the number of transmitters. Unfortunately, real source separation problems do not always satisfy this constraint. In fact, the number of transmitters is often greater than the number of receivers (i.e., an over-complete ICA). The algorithms used for over-complete ICA are based on the guiding assumption that source signals are sparse[16]. Since this assumption doesn't hold in our case, overcomplete ICA algorithms cannot be used to solve our hypothetical problem. Hence, new techniques or algorithms should be introduced to solve a multi-user communication problem when the number of transmitters is greater than the number of receivers.

Furthermore, future work will extend results obtained with ICA in other applications. For example, the ICA algorithm can be leveraged for sensing in a cognitive free space link. Although the number of source signals must be known to perform the ICA algorithm, the number of users can change dynamically. Hence, receiver can be used to estimate the number of users attempting to transmit information and several estimation techniques have been proposed[7]. This proposed work warrants further exploration, despite the work detailed in this paper proves that the ICA algorithm is a valuable and promising unsupervised technique to accomplish such a goal.

REFERENCES

[1] M. A. Khalighi and M. Uysal, "Survey on Free Space Optical Communication: A Communication Theory Perspective," *IEEE Commun. Surv. Tutorials*, vol. 16, no. 4, pp. 2231–2258, 2014.

[2] H. Kaushal and G. Kaddoum, "Optical communication in space: Challenges and mitigation techniques," *IEEE*

Commun. Surv. Tutorials, vol. 19, no. 1, pp. 57–96, 2017.

[3] P. LoPresti, N. Hutchins, S. Kohrmann, M. F. Babelli, and H. H. Refai, "Wavelength dependence of a fiber-bundle based FSO link," in *Globecom Workshops (GC Wkshps), 2014*, 2014, pp. 493–498.

[4] T. Rakia, F. Gebali, H.-C. Yang, and M.-S. Alouini, "Throughput analysis of point-to-multi-point hybric FSO/RF network," in *Communications (ICC), 2017 IEEE International Conference on*, 2017, pp. 1–6.

[5] P. Comon and C. Jutten, *Handbook of Blind Source Separation: Independent component analysis and applications*. Academic press, 2010.

[6] A. Hyvärinen and E. Oja, "Independent component analysis: algorithms and applications," *Neural networks*, vol. 13, no. 4, pp. 411–430, 2000.

[7] Z. Uddin, A. Ahmad, M. Iqbal, and M. Naeem, "Applications of independent component analysis in wireless communication systems," *Wirel. Pers. Commun.*, vol. 83, no. 4, pp. 2711–2737, 2015.

[8] T.-W. Lee, M. Girolami, and T. J. Sejnowski, "Independent component analysis using an extended infomax algorithm for mixed subgaussian and supergaussian sources," *Neural Comput.*, vol. 11, no. 2, pp. 417–441, 1999.

[9] J. R. Hershey and P. A. Olsen, "Approximating the Kullback Leibler divergence between Gaussian mixture models," in *Acoustics, Speech and Signal Processing, 2007. ICASSP 2007. IEEE International Conference on*, 2007, vol. 4, p. IV-317.

[10] D. N. Rutledge and D. J.-R. Bouveresse, "Independent components analysis with the JADE algorithm," *TrAC Trends Anal. Chem.*, vol. 50, pp. 22–32, 2013.

[11] F. Aveta, H. H. Refai, and P. LoPresti, "Multi-user FSO communication link," in *2017 Cognitive Communications for Aerospace Applications Workshop (CCAA)*, 2017, pp. 1–5.

[12] P. Xie and S. L. Grant, "A Fast and Efficient Frequency-Domain Method for Convolutive Blind Source Separation," in *2008 IEEE Region 5 Conference*, 2008, pp. 1–4.

[13] A. Hyvarinen, "Fast and robust fixed-point algorithms for independent component analysis," *IEEE Trans. Neural Networks*, vol. 10, no. 3, pp. 626–634, 1999.

[14] H. Kasturiwale and Z. Mizwan, "Comparison and Performance Analysis of various ICA Algorithms for ECG signals," *Int. J. Eng. Res. Technol.*, vol. 3, no. 4, 2014.

[15] D. Vigliano, M. Scarpiniti, R. Parisi, and A. Uncini, "Flexible ICA approach to the nonlinear blind signal separation in the complex domain," in *2006 14th European Signal Processing Conference*, 2006, pp. 1–5.

[16] G. R. Naik and D. K. Kumar, "An overview of independent component analysis and its applications," *Informatica*, vol. 35, no. 1, 2011.